Multiple slip effects on dissipative and chemical reactive MHD flow over a permeable stretching sheet in the presence of heat source

Bharat Keshari Swain

Agarpara College, Agarpara, Bhadrak, Odisha, 756115, India

bharatkeshari1@gmail.com

Abstract: The present investigation construes the unsteady MHD flow over a permeable stretching sheet embedded in a porous medium. The effects of viscous and Darcy dissipation, heat source and chemical reaction have been delineated with the existence of multiple slips. Similarity variables are employed for remodeling the governing equations as a system of first order nonlinear ordinary differential equations. The reduced system is dealt with 4^{th} order Runge-Kutta method along with shooting technique. The present results have been verified with earlier works and found a good agreement. The important findings reported herein are: porosity acts as aiding force for the fluid velocity, more dissipative heat leads to higher velocity and temperature, chemical reaction parameter adversely affects the concentration. This analysis is relevant to various industrial processes at boundaries of pipes, walls, and/or curved surfaces.

Keywords: Viscous dissipation, Darcy dissipation, Heat source, Chemical reaction, multiple slips.

Nomenclature:

a	Stretching rate	D_T	Thermal diffusivity

21	B_0	Magnetic field of constant strength	E_c	Eckert number
22	C	Concentration of the fluid	f_w	Suction/injection
23	C_f	Local skin friction coefficient	k^*	Mean absorption coefficient
24	Cfr	Reduced skin friction	K_p	Porosity parameter
25	C_p	Specific heat	M	Magnetic field parameter
26	C_o	Reference concentration	Nur	Reduced Nusselt Number
27	C_w	Stretching sheet concentration	P_r	Prandtl number
28	C_∞	Ambient concentration	Q	Heat source parameter
29	D_d	Darcy dissipation parameter	R_c	Chemical reaction parameter
30	D_M	Molecular diffusivity	Re_x	Local Reynolds number
31	S_c	Schmidt number	ϕ	Nondimensional concentration
32	S_f	Velocity slip	η	Similarity variable
33	Shr	Reduced Sherwood number	ν	Kinematic viscosity
34	S_r	Soret number	α	Thermal diffusivity
35	S_θ	Thermal slip	β_C	Concentration expansion coefficient
36	S_ϕ	Solutal slip	β_T	Thermal expansion coefficient
37	T	Temperature	τ	Stress tensor

38	T_w	Stretching sheet temperature	δ	Unsteady parameter
39	T_0	Reference temperature	λ	Constant
40	T_∞	Ambient temperature	ρ	Density
41	u	x component of velocity	λ_1	Thermal buoyancy parameter
42	v	y component of velocity	λ_2	Solutal buoyancy parameter
43	x,y	Coorinates	σ^*	Stefan-Boltzmann constant

44 **Greek Symbol:**

45	θ	Non-dimensional temperature

46 **1. Introduction:**

47 Magnetohydrodynamics (MHD) may be described as the microscopic interaction of
48 electrically conducting fluid and magnetic field. Its application ranges from industries to space
49 science as well as magnetic-therapy. In recent years, MHD flow with the slip condition is of
50 engineering interest. If the viscous force between liquid molecules at the interface is stronger
51 than the force between the molecules of the liquid and molecules of the solid, then the molecules
52 can slide on the surface. The resemblance of the mean free path of particles with the flow field
53 characteristic gives rise to the breakdown of Navier-Stokes equations because the hypothesis of
54 continuum media fails. If the Knudsen number (Kn) remains in 1< Kn < 10, the higher order
55 continuum equation like Burnett equation is appropriate. No-slip condition can't be used (Hak,
56 1999) in the range of 0.1 > Kn >0.001. For Kn < 0.001, the no-slip condition is authentic.

Particularly, in case of emulsions, suspensions etc., no-slip condition is insufficient and slip could occur on the boundary.

The fluid flow nature under slip condition deviates from the standard flow. The slip flows under various configurations were inspected by several researchers. Raza, Rohni, Omar and Awais (2016) illuminated the performance of slip in a nanofluid flow during rotating channel. Turkyilmazoglu (2013) did the mass transfer analysis in a slip flow of fluid. Akbar and Khan (2014) have studied the impact of thermal as well as velocity slips on biviscosity fluid flow. Hayat, Awais and Hendi (2012) and Reddy (2016) elucidated the impact of slip condition on rotating flow between two porous walls and on MHD peristaltic flow respectively. Mabood & Shateyi (2019) studied radiative MHD unsteady flow with multiple slips. Swain, Biswal and Dash (2021) have investigated the second order slip effect and heat source on dissipative MHD flow of blood through a permeable capillary in stretching motion. They found that skin friction coefficient at the capillary wall decreases with higher order slip.

Application of external magnetic field in various MHD flow problems is considerably vital. When this flow is considered trough a porous medium, then study becomes more alluring. These forms of engineering issues are more admissible in energy extractions, oil exploration and also the physical phenomenon management within the field of aeromechanics. So several investigations are explored by the celebrated researchers. Sekhar, Reddy, Raju, Ibrahim and Makinde (2018) illustrated the multiple slips impacts on MHD flow through porous medium. Makinde, Khan, Ahmad and Khan (2018) studied unsteady hydromagnetic radiating fluid flow past a slippery stretching sheet embedded in a porous medium. Makinde, Khan and Khan (2016) analyzed the MHD nanofluid flow over a convectively heated permeable vertical plate embedded in a porous medium. Mutuku-Njane and Makinde (2013) illuminated the ramification of MHD

flow of a nanofluid over a convectively heated vertical porous plate through porous medium. Swain and Senapati (2015) inspected the effect of mass transfer on free convective flow set in a porous medium in the presence of magnetic field. Uddin (2015) has also made his analysis considering magnetic field and a porous medium.

The internal energy in the fluid element is modified by the flow of heat and also the performance of work. The work done consists of the reversible half and dissipated work. we tend to solely take into account the contribution from the mechanically dissipated energy per unit volume (SI unit W/m3), effort aside the contribution of the entropy flux and also the production of entropy stems from the finite temperature distinction in thermal conductivity (Baehr and Stephan (2006)). Anjali and Ganga (2010) investigated the outcome of dissipation for a nonlinear flow with prescribed heat flux. Ferdows, Chapal and Afify (2014) expounded the nanofluid flow considering permeable stretching sheet and clearly discussed the result of viscous dissipation. Venkateswarlu, Satya Narayana and Tarakaramu (2018) investigated the viscous dissipation response on MHD flow over a moving surface with constant heat supply. Hunegnaw and Kishan (2017) elucidated on the repercussion of viscous dissipation in an unsteady MHD flow over stretching sheet. Biswal, Swain, Das and Dash (2022) studied the effect of viscous dissipation in their study of MHD stagnation point flow towards an inclined stretching sheet embedded in a porous medium. Swain, Parida, Kar and Senapati (2020) investigated viscous dissipation and joule heating effect on MHD flow and heat transfer past a stretching sheet embedded in a porous medium. Parida, Swain and Senapati (2021) analyzed viscous dissipative MHD nanofluid flow over a stretching sheet embedded in a porous medium.

Chemical reaction is additionally of extended importance in fluid flow at the side of the combined impact of heat and mass transfer. These kinds of studies have large utilizations

in several industrial processes and conjointly in physiological flows. Reaction is called to be homogeneous once it happens uniformly through a given part. Otherwise reaction is termed as heterogeneous. Further, chemical reaction is of first order if rate of reaction is directly proportional to the concentration. Possible applications may be found in processes like drying, injury of crops because of state change, water surface evaporation etc. Several researchers have done their research analysis regarding this subject. Chamber and Young (1958) delineated the consequences of homogeneous first order chemical reactions within the neighborhood of a flat plate. Muthucumaraswamy and Janakiramana (2008) and Swain , Senapati and Dash (2014) have studied the impact of chemical change in MHD physical boundary layer flow past a vertical plate. Ahmed (2014) and Ahmed and Kalita (2014) resolved numerically the MHD flow issues taking care of chemical reaction. Swain, Senapati and Dash (2017) have conjointly given their interest on resolution the matter of chemical reaction effect on free convective Flow. Swain (2021) has also shown his interest on solving the problem of second order chemical reaction effect on MHD convective flow. He explained the consequences of the second order chemical reaction after solving the pertinent equations by finite difference method.

The above studies and applications show the importance of dissipative and chemical reactive MHD flow in the presence of multiple slips. Fluid flow through porous medium and Darcy dissipation, which stems from the resistance offered by viscosity of the fluid and porous matrix of the saturated porous medium are analyzed here. This type of flow is very applicable in irrigation and drainage problems, extraction of particulates from soil, cosmetic and petrochemicals products etc. Further, heat source due to temperature difference which provides thermal power to heat transfer process may be of possible occurrence. The above aspects are not

considered by Mabood and Shateyi (2019) and Mabood and Das (2016). This research gap motivates the present study.

The novelties of the present study are:

(i) to study the effects of viscous and Darcy dissipation on MHD flow through porous medium.

(ii) to analyze the influence of heat source and chemical reaction.

(iii) to analyze the flow with multiple slip conditions.

(iv) to discuss the works of Mabood & Shateyi (2019), Mabood & Das (2016) , Chamkha, Aly and Mansour (2010) and Ali (1994) as particular cases.

2. Mathematical Formulation:

Present analysis deals with a permeable surface along which the *x*-axis is taken. The *y*-axis is drawn normal to x-axis. The fluid flows over a permeable stretching sheet embedded in a porous medium. The sheet is stretched with velocity $U_w(x,t)=\frac{ax}{1-\lambda t}$ in the direction of x-axis. Magnetic field $B(t)=B_0(1-\lambda t)^{-1/2}$ is applied in transverse direction and B_0 is constant initial magnetic field strength. Figure.1 depicts the present flow system. The induced magnetic field is negligible. T_∞ and C_∞ are taken as the ambient temperature and mass concentration respectively. Since the wall is permeable, so multiple slips are analyzed.

The following points are assumed in the present analysis.

(i) The two dimensional viscous flow is unsteady, incompressible, free convective and electrically conducting.

(ii) The stretching permeable sheet is subjected to transverse magnetic field and embedded in porous medium.

(iii) There exist velocity slip, thermal slip as well as solutal slip.

(iv) The induced magnetic field is neglected.

(v) It is also assumed that no polarization voltage exists.

(vi) The diffusive species is chemically reactive with variable concentration at the surface.

The governing equations are conferred as (cf. Mabood & Shateyi (2019), Misra &Sinha (2013))

$$\frac{\partial u}{\partial x}+\frac{\partial v}{\partial y}=0 \quad , \tag{1}$$

$$\frac{\partial u}{\partial t}+u\frac{\partial u}{\partial x}+v\frac{\partial u}{\partial y}=\nu\frac{\partial^2 u}{\partial y^2}-\left(\frac{\sigma B^2(t)}{\rho}+\frac{\nu}{K_p^{\,*}(t)}\right)u+g\beta_T(T-T_\infty)+g\beta_C(C-C_\infty) \quad , \tag{2}$$

$$\frac{\partial T}{\partial t}+u\frac{\partial T}{\partial x}+v\frac{\partial T}{\partial y}=\alpha\left(1+\frac{16{T_\infty}^3\sigma^*}{3k^*k}\right)\frac{\partial^2 T}{\partial y^2}+\frac{\mu}{\rho C_p}\left(\frac{\partial u}{\partial y}\right)^2+\frac{\mu}{\rho C_p K_p^{\,*}(t)}u^2+\frac{Q^*}{\rho C_p}(T-T_\infty), \tag{3}$$

$$\frac{\partial C}{\partial t}+u\frac{\partial C}{\partial x}+v\frac{\partial C}{\partial y}=D_M\frac{\partial^2 C}{\partial y^2}+D_T\frac{\partial^2 T}{\partial y^2}-R_c^{\,*}(C-C_\infty) \quad . \tag{4}$$

The boundary conditions are given by

$$\begin{cases} y=0: u=U_w(x,t)+U_{slip}, v=V_w, \\ T_w(x,t)+T_{slip}, C_w(x,t)+C_{slip} \\ y\to\infty: u\to 0, T\to T_\infty, C\to C_\infty \end{cases} \quad . \tag{5}$$

Sheet temperature $T_w(x,t)$ and concentration $C_w(x,t)$ at the surface are taken as

$$T_w(x,t)=T_\infty+T_0\left(\frac{ax}{2\nu}\right)(1-\lambda t)^{-2}, C_w(x,t)=C_\infty+C_0\left(\frac{ax}{2\nu}\right)(1-\lambda t)^{-2} \tag{6}$$

where T_0 , the reference temperature and C_0 , the reference concentration and $0\le T_0\le T_W$, $0\le C_0\le C_W$. The above expressions are valid for $(1-\lambda t)>0$.

In equations (2) and (3), $K_p^{\,*}(t)=k_1(1-\lambda t)$ is the time dependent permeability parameter.

In (5), V_w represents injection/suction velocity of fluid at the surface and is given by

$$V_w=-\sqrt{\frac{a\nu}{1-\lambda t}}f(0).$$

165 The stream function ψ is expressed as $u = \frac{\partial \psi}{\partial y}$ and $v = -\frac{\partial \psi}{\partial x}$ that satisfy equation (1). The non-

166 dimensional functions and variable f, θ, ϕ and η are taken as follows:

$$\eta = \sqrt{\frac{a}{\nu(1-\lambda t)}}y, \psi = \sqrt{\frac{a\nu}{(1-\lambda t)}}xf(\eta), T = T_\infty + T_0\left(\frac{ax(1-\lambda t)^{-2}}{\nu}\right)\theta(\eta),$$

167 $$C = C_\infty + C_0\left(\frac{ax(1-\lambda t)^{-2}}{\nu}\right)\phi(\eta) \quad . \qquad (7)$$

168 Now putting (7) in equations (2)-(4), following equations are obtained

169 $$f''' + ff'' - f'^2 - \delta\left(\frac{\eta}{2}f'' + f'\right) - \left(M + \frac{1}{K_p}\right)f' + \lambda_1\theta + \lambda_2\phi = 0 \quad , \qquad (8)$$

170 $$\frac{1}{P_r}(1+R)\theta'' + f\theta' - f'\theta - \delta\left(\frac{\eta}{2}\theta' + 2\theta\right) + E_c f''^2 + D_d f'^2 + Q\theta = 0 \quad , \qquad (9)$$

171 $$\phi'' + S_c(f\phi' - f'\phi) - S_c\delta\left(\frac{\eta}{2}\phi' + 2\phi\right) + S_c S_r\theta'' - S_c R_c\phi = 0 \quad . \qquad (10)$$

172 The reduced boundary conditions are

173 $$\begin{aligned} &f(0) = f_w,\ f'(0) = 1 + S_f f''(0), \theta(0) = 1 + S_\theta\theta'(0), \phi(0) = 1 + S_\phi\phi'(0), \\ &f'(\infty) = 0, \theta(\infty) = 0, \phi(\infty) = 0. \end{aligned} \qquad (11)$$

174 The non-dimensional parameters used in (8)-(11) are given by

175 $$\delta = \frac{\lambda}{a}, \lambda_1 = \frac{g\beta_T T_0}{a\nu}, \lambda_2 = \frac{g\beta_C C_0}{a\nu}, P_r = \frac{\nu}{\alpha}, R = \frac{16T_\infty^{\ 3}\sigma^*}{3k^*k}, M = \frac{\sigma B_0^{\ 2}}{\rho a}, K_p = \frac{ak_1}{\nu}, S_c = \frac{\nu}{D_M}$$
$$S_r = \frac{D_T T_0}{\nu C_0}, f_w = -V_w\sqrt{\frac{1-\lambda t}{\nu a}}, D_d = \frac{E_c}{K_p}, E_c = \frac{U_w^{\ 2}}{C_p(T_w - T_\infty)}, Q = \frac{Q^*(1-\lambda t)}{\rho C_p a}, R_c = \frac{R_c^{\ *}(1-\lambda t)}{a}$$

176 $S_f = A_1\sqrt{\frac{a}{\nu(1-\lambda t)}}, S_\theta = A_2\sqrt{\frac{a}{\nu(1-\lambda t)}}, S_\phi = A_3\sqrt{\frac{a}{\nu(1-\lambda t)}}$.

177 A_1, A_2, A_3 are velocity slip factor, thermal slip factor and solutal slip factor respectively.

178 $A_1 = A_2 = A_3 = 0$, gives no slip conditions.

179 Here, $f_w = 0$ represents the impermeable surface, $f_w > 0$ produce suction and $f_w < 0$ means

180 injection.

181 The physical quantities local skin friction coefficient C_f, local Nusselt number Nu and local

182 Sherwood number Sh are defined as

183 $$C_f = \frac{\mu}{\rho U_w^{\,2}}\left(\frac{\partial u}{\partial y}\right)_{y=0}, \tag{12}$$

184 $$Nu = -\frac{x}{k(T_W - T_\infty)}\left[k\left(\frac{\partial T}{\partial y}\right)_{y=0} - \frac{4\sigma^*}{3k^*}\left(\frac{\partial T^4}{\partial y}\right)_{y=0}\right], \tag{13}$$

185 $$Sh = -\frac{x}{(C_W - C_\infty)}\left(\frac{\partial C}{\partial y}\right)_{y=0}. \tag{14}$$

186 Putting (7) into equations (12)-(14), the non-dimensional forms obtained are:

187 $$Cfr = \sqrt{\mathrm{Re}_x}C_f = f''(0), Nur = \frac{Nu}{\sqrt{\mathrm{Re}_x}} = -(1+R)\theta'(0), Shr = \frac{Sh}{\sqrt{\mathrm{Re}_x}} = -\phi'(0), \tag{15}$$

188 **3. Method of Solution**:

189 The coupled nonlinear equations (8) - (10) under the boundary conditions (11) have been worked

190 out using the fourth order Runge-Kutta method with shooting technique. The equations (8)-(10)

have been converted to a set of first order differential equation substituting

$$f = y_1, f' = y_2, f'' = y_3, \theta = y_4, \theta' = y_5, \phi = y_6, \phi' = y_7 . \quad (16)$$

The reduced equations are

$$y_3' = -y_1 y_3 + {y_2}^2 + \delta\left(y_2 + \frac{1}{2}\eta y_3 \right) + \left(M + \frac{1}{K_p} \right) y_2 - \lambda_1 y_4 - \lambda_2 y_6, \quad (17)$$

$$y_5' = \left(\frac{\Pr}{1+R} \right)\left(-y_1 y_5 + y_4 y_2 + \delta\left(2y_4 + \frac{1}{2}\eta y_5 \right) - E_c {y_3}^2 - D_d {y_2}^2 - Q y_4 \right), \quad (18)$$

$$y_7' = -S_c\left(y_1 y_7 - y_2 y_6 \right) + S_c \delta\left(2y_6 + \frac{\eta}{2} y_7 \right) - S_c S_r y_5' + S_c R_c y_6 \quad (19)$$

Boundary conditions are written as

$$y_1 = f_w, y_2 = 1 + S_f y_3, y_3 = ?, y_4 = 1 + S_\theta y_5, y_5 = ?, y_6 = 1 + S_\phi y_7, y_7 = ? \text{ at } \eta = 0, \quad (20)$$

$$y_2 \to 0, y_4 \to 0, y_6 \to 0 \quad \text{as} \quad \eta \to \infty . \quad (21)$$

For integration, the values of y_3, y_5 and y_7 at $\eta = 0$ are guessed and the step by step integration is accomplished with step length 0.01 adopting shooting technique with MATLAB code having error bound 10^{-3}.

4. Validation: To validate the present results, the previous studies are taken into account in Tables.1, 2 and 3. Table.1 and Table.2 give the values of skinfriction of previous studies (Chamkha, Aly & Mansour (2010), Mabood and Shateyi (2019), Mabood and Das (2016)) and present results for unsteady parameter and magnetic field parameter respectively. Similarly, some values of Nusselt numer of the present study for Prandtl number are compared to that of

the previous studies (Mabood and Shateyi (2019), Ali (1994)) in Table.3. It is found that the present results are in good agreement with the earlier studies, which shows the accuracy of the present study.

5. Results and Discussion: Numerical solutions to an unsteady MHD flow over permeable stretching sheet with multiple slip effects embedded in a porous medium are obtained. The effects of viscous and Darcy dissipation, heat source and chemical reaction are of main concern. The values of pertinent parameters are considered following Mabood and Shateyi (2019) and Mabood and Das (2016). The repercussion of physical parameters are elucidated through graphs and tables assuming the parameters as

$$P_r = 1, S_c = 10, \lambda_1 = \lambda_2 = 0.2, M = 1, S_\theta = S_\phi = S_r = R = 0.5, \delta = 0.2, f_w = 1, S_f = 1, E_c = 0.2,$$
$$Q = 0.5, K_p = 1, R_c = 0.5$$

unless or otherwise stated.

Figure.2 illustrates the effect of heat source parameter Q on velocity. It is obtained that the increasing values of Q enhance the velocity. Again it displays the effect of no-slip and first order velocity slip on velocity distribution. It is observed that the decrease in velocity commensurates with the order of slip. This can be attributed to low momentum transport/diffusion within the boundary layer.

In Fig.3, porosity parameter K_p acts as aiding force for the fluid velocity i.e. the increasing values of K_p enhance the velocity. This is because with a rise in permeability of the medium, the regime becomes more porous. As a consequence, the Darcian body force decreases the magnitude (as it is increasing proportional to the permeability). The Darcian resistance acts to decelerate the fluid particles in continuous. This resistance diminishes as permeability of the medium increases. So progressively less drag is experienced by the flow and flow retardation is

there by decreased. Hence, the velocity of the fluid increases as the permeability parameter increases. On careful observation, again it is found that when K_p is increased from 0.1 to 1, rate of change in velocity is higher and after that rate of increment gets slowdown in the range of K_p= 1 to10. Again, it is found that velocity slip leads a lower velocity.

Figure.4 elucidates the impacts of Eckert number (E_c) on velocity distribution respectively. The parameter is directly proportional to the velocity. As Eckert number comes from kinetic energy of flow and heat enthalpy difference, so improve in Eckert number enhances kinetic energy. Again it is known that temperature is considered as average kinetic energy. Greater viscous dissipative heat rises the temperature. Thus we can say that temperature of the fluid rises. From the Figure.6, it is analyzed that fluid temperature rises as E_c is increased. Due to higher temperature, resistive power to the fluid flow reduces and fluid moves with higher velocity (in fig. 6) for higher values of E_c .

In Figure.5, Temperature profiles are drawn for various values of porosity parameter K_p. Increase in both the parameters helps to fall in temperature significantly with and without thermal slip. In case of no thermal slip (S_θ =0), temperature is comparatively more.

As heat supply is increased, temperature rises across the flow field Figure.7. Consequently, it yields a thicker thermal boundary layer. It is pertinent to notice that Q measures internal thermal power per unit volume of the fluid. An increase in heat source means an increase in thermal power. It also gives rise to lower temperature for first order thermal slip as compared to no-slip condition. Moreover, with increase in temperature the fluid gets thin and becomes less viscous. Therefore the fluid flows with higher velocity.

Figure.8 delineate the impact Chemical reaction parameter (R_c) on concentration profile respectively. It is observed that larger values of Chemical reaction parameter lead to lower

concentration. This is due to the fact that destructive chemical reduces the solutal boundary layer thickness and increases the mass transfer. In physical point of view chemical reaction for destructive case is very large. Because of this fact molecular motion is quite higher which enhances the transport phenomenon, thus suppressing the concentration field in the fluid flow. This figure also confirms that decrease in concentration commensurate with the order of solutal slip.

Table-4 represents the effects of λ_1, λ_2, K_p, E_c, Q, R_c and S_c on skin friction , Nusselt number and Sherwood number. The other parameters are taken as $P_r = 1, S_f = 0.2, \delta = M = 0.5, R = S_\theta = S_\phi = S_r = 0.5, f_w = 0.2$. It is observed that increasing values of λ_1, λ_2, and K_p simultaneously increase skin friction coefficient and improve the rate of heat and mass transfer. This results show a good agreement with the results of Mabood and Shateyi(2019). Further, it is noticed that higher values of E_c and Q help to increase the skin friction but reverse trend is shown in case of R_c and S_c.

Now higher values of E_c are obtained small temperature difference and so rate of heat transfer decreases. Similarly more the heat source parameter, Q less the rate of heat transfer. Likewise, increase in R_c and S_c leads to the heat transfer rate. Finally rate of mass transfer is analyzed. It is noted that all the parameters are directly proportional to rate of mass transfer.

6. Conclusion: The present study reveals the chemical reactive and dissipative MHD flow over a permeable stretching sheet embedded in a porous medium in the presence of heat source. The governing equations are solved using similarity transformation and Runge-Kutta method of

fourth order along with shooting technique. The results are analyzed through graphs and tables. Some of the conclusions are drawn from the results as follows:

- Higher values of heat source parameter enhance the velocity.
- Porosity parameter performs as an aiding force for the velocity of fluid.
- Fluid moves with higher velocity for higher values of viscous dissipation parameter.
- Higher values of chemical reaction parameter reduce the velocity of the fluid flow.
- Increasing values of dissipative heat represented by Ec, because of viscous dissipation gives rise to significant increase in temperature.
- Increase in porosity helps to fall in temperature significantly with and without thermal slip.
- Larger values of Chemical reaction parameter lead to lower concentration. Higher values of E_c and Q lead to increase the skin friction but reverse trend is shown in case of R_c and S_c.

The limitation of the present study are:

(i) the joulean dissipation, which is generated because of outwardly magnetic field interacting with conducting liquid, has been neglected .

(ii) induced magnetic field and hall current are neglected which should be studied in case of strong applied magnetic field strength.

The above limitations may be studied and considered as future directions for research. Effect of second slip conditions may also be taken care of and flow may be considered over different type of surfaces like wavy surface.

References:

Ahmed, S. (2014)., Numerical analysis for magneto hydrodynamic chemically reacting and radiating fluid past a non-isothermal impulsively started vertical surface adjacent to a porous regime. Ain Shams Engineering Journal, 5, 923-933.

Ahmed, S. & Kalita, K. (2014). Unsteady MHD chemically reacting fluid through a porous medium bounded by a non-isothermal impulsively-started vertical plate: A numerical technique. Journal of Naval Architecture and Marine Engineering, 11, 39-54.

Akbar, N.S. & Khan, Z.H. (2014). Heat transfer analysis of the peristaltic instinct of biviscosity fluid with the impact of thermal and velocity slips. International Communications in Heat and Mass Transfer, 58, 193- 199.

Ali, M. E. (1994). Heat transfer characteristics of a continuous stretching surface. Warme-und Stoffubertragung, 29, 227-234.

Anjali Devi, S .P. & Ganga, B. (2010). Dissipation Effects on MHD Nonlinear Flow and Heat Transfer Past a Porous Surface with Prescribed Heat flux. Journal of Applied Fluid Mechanics, 3, 1-6.

Baehr, H. D. & Stephan, K. (2006). Heat and Mass transfer, 2nd edition, Springer, pp-280.

Biswal, M.M., Swain, B.K., Das, M. & Dash, G.C. (2022), Heat and Mass transfer in MHD stagnation point flow towards an inclined stretching sheet embedded in a porous medium. Heat Transfer, 51, 4837-4857.

Chamber, P. L. & Young, J. D. (1958). The effects of homogeneous 1st order chemical reactions in the neighbourhood of a flat plate for destructive and generative reactions. Physics of Fluids, 1, 48-54.

Chamkha, A. J. , Aly, A. M. & Mansour, M. A. (2010). Similarity solution for unsteady heat and mass transfer from a stretching surface embedded in a porous medium with suction/injection and chemical reaction effects. Chemical Engineering Communications, 197, 846-858.

Ferdows, M. , Chapal, S.M. & Afify, A.A. (2014). Boundary layer flow and heat transfer of a nanofluid over a permeable unsteady stretching sheet with viscous dissipation. Journal of Engineering Thermophysics, 23, 216-228.

Gad-el-Hak (1999). The fluid mechanics of micro devices - the freeman scholar lecture, ASME. Journal of Fluids Engineering, 121, 5-33.

Hayat, T., Awais, M. & Hendi, A.A. (2012). Three-dimensional rotating flow between two porous wall with slip and heat transfer. International Communications in Heat and Mass Transfer, 39, 551-555.

Hunegnaw, D. & Kishan, N. (2017). Unsteady MHD heat and mass transfer flow over stretching sheet in porous medium with variable properties considering viscous dissipation and chemical reaction. American Chemical Science Journal, 4, 901-917.

Mabood, F. & Das, K. (2016). Melting heat transfer on hydromagnetic flow of a nanofluid over a stretching sheet with radiation and second-order slip. The European Physical Journal Plus, vol. 131, 1-12.

Mabood, M. & Shateyi, S. (2019). Multiple slip effects on MHD unsteady flow heat and mass transfer impinging on permeable stretching sheet with radiation. Modelling and Simulation in Engineering, 2019, 1-11.

Makinde, O. D., Khan, W.A. & Khan, Z.H. (2016). Analysis of MHD nanofluid flow over a convectively heated permeable vertical plate embedded in a porous medium. Journal of Nanofluids 5, 574-580.

Makinde, O. D., Khan, Z.H., Ahmad, R. & Khan, W. A. (2018). Numerical study of unsteady hydromagnetic radiating fluid flow past a slippery stretching sheet embedded in a porous medium. Physics of Fluids, 30, 083601-083607.

Misra, J.C. & Sinha, A. (2013). Effect of thermal radiation on MHD flow of blood and heat transfer in a permeable capillary in stretching motion. Heat Mass Transfer, 49, 617-628.

Muthucumaraswamy, R. & Janakiramana, B. (2008). Mass transfer effect on isothermal vertical oscillating plate in presence of chemical reaction. International Journal of Applied Mathematics and Mechanics, 4, 66-74.

Mutuku-Njane, W. N. & Makinde, O. D. (2013). Combined effect of buoyancy force and Navier Slip on MHD flow of a nanofluid over a convectively heated vertical porous plate. The Scientific World Journal, 2013, 1-8.

Parida, B.C., Swain, B.K., Senapati, N. (2021). Mass transfer effect on viscous dissipative MHD flow of nanofluid over a stretching sheet embedded in a porous medium. Journal of Naval Architecture and Marine Engineering, 18, 73-82.

Raza, J., Rohni, A.M., Omar, Z. & Awais, M. (2016). Heat and mass transfer analysis of MHD nanofluid in a rotating channel with slip effects. Journal of Molecular Liquids, 219, 703-708.

Reddy, M.G. (2016). Heat and mass transfer on Magnetohydrodynamic peristaltic flow in a porous medium with partial slip. Alexandria Engineering Journal, 55, 1225-1234.

Sekhar, K.R., Reddy, G.V., Raju, C.S.K., Ibrahim, S.M. & Makinde, O.D. (2018). Multiple slip effects on magnetohydrodynamic boundary layer flow over a stretching sheet embedded in a porous medium with radiation and joule heating. Special Topics & Reviews in Porous media: An International journal, 9, 117-132.

Swain, B. K. (2021). Effect of second order chemical reaction on MHD free convective radiating flow over an impulsively started vertical plate. Journal of Nonlinear Modelling and Analysis, 3, 167-178.

Swain, B.K., Biswal, M.M. & Dash, G.C. (2021). Effect of the second-order slip and heat source on dissipative MHD flow of blood through a permeable capillary in stretching motion. International Journal of Ambient Energy, DOI: 10.1080/01430750.2021.1979649.

Swain, B.K., Parida, B.C., Kar, S. & Senapati, N.(2020). Viscous dissipation and joule heating effect on MHD flow and heat transfer past a stretching sheet embedded in a porous medium. Heliyon, 6, 1-8. https://doi.org/10.1016/j.heliyon.2020.e05338

Swain, B. K. & Senapati, N. (2015). The effect of mass transfer on MHD free convective radiating flow over an impulsively started vertical plate embedded in a porous medium. Journal of Applied Analysis and Computation, 5, 18-27.

Swain, B. K., Senapati, N. & Dash, M. (2014). The effect of chemical reaction and thermal radiation on the hydromagnetic free convective rotating flow past an accelerated vertical plate in the presence variable heat and mass diffusion. Der Chemica Sinica, 5, 56-66.

Swain, B.K., Senapati, N. & Dash, M. (2017). Chemical Reaction Effect on MHD Convective Flow with Heat and Mass Transfer Past a Semi-Infinite Vertical Porous Plate. Journal of Advanced Mathematics and Applications, 6, 1-8.

Turkyilmazoglu, M. (2013). Heat and mass transfer of MHD second order slip flow. Computers and Fluids, 71, 426-434.

Uddin, M. S. (2015).Viscous and Joules Dissipation on MHD Flow past a Stretching Porous Surface Embedded in a Porous Medium. Journal of Applied Mathematics and Physics, 3, 1710-1725.

Venkateswarlu, B., Satya Narayana, P.V., & Tarakaramu, N. (2018). Melting and Viscous dissipation effects on MHD flow over a moving surface with constant heat source. Transactions of A.Razmadze Mathematical Institute, 172, 618-630.

Figure

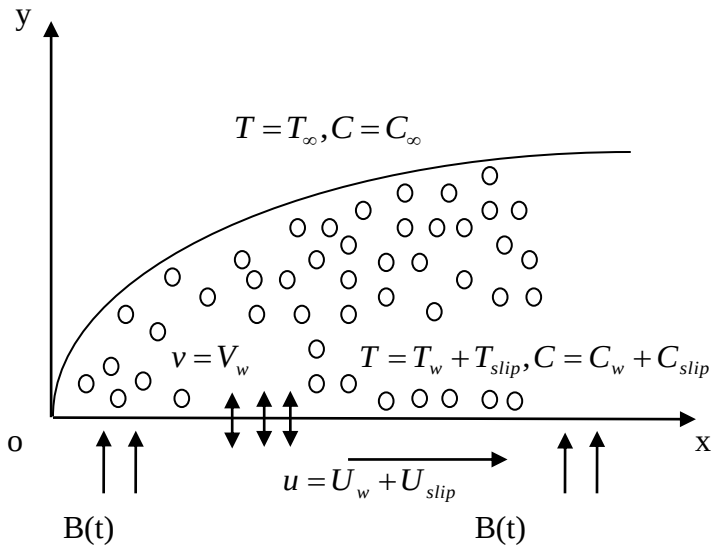

Figure.1. Physical problem

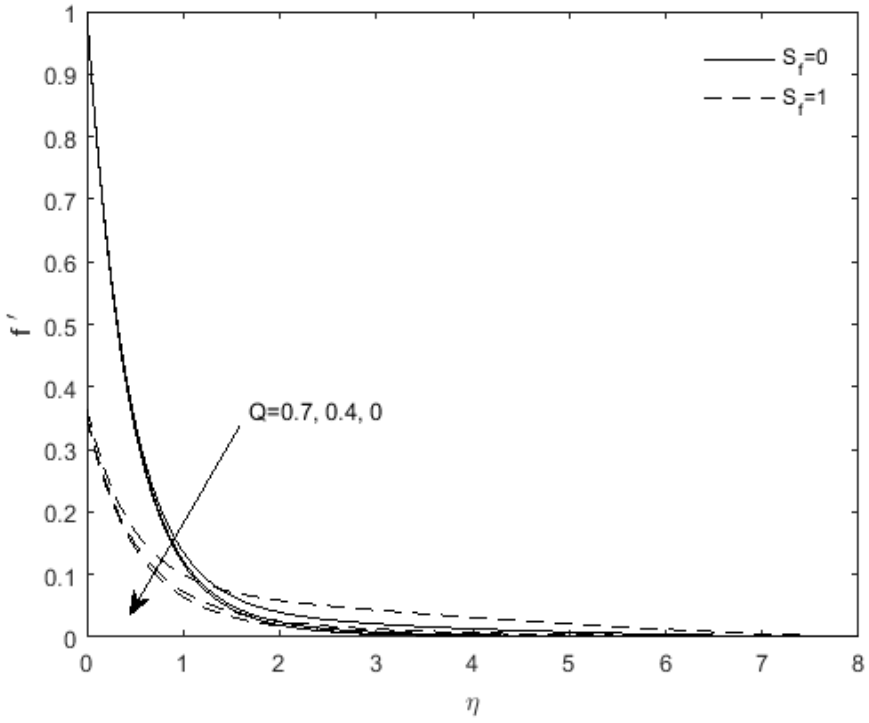

Fig.2. Velocity profile for Q

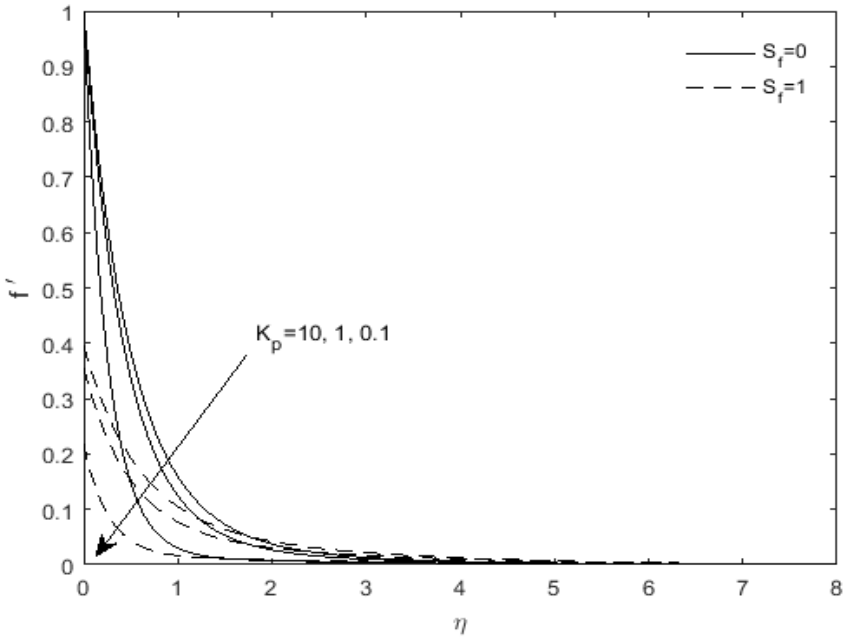

Fig.3. Velocity profile for K_p

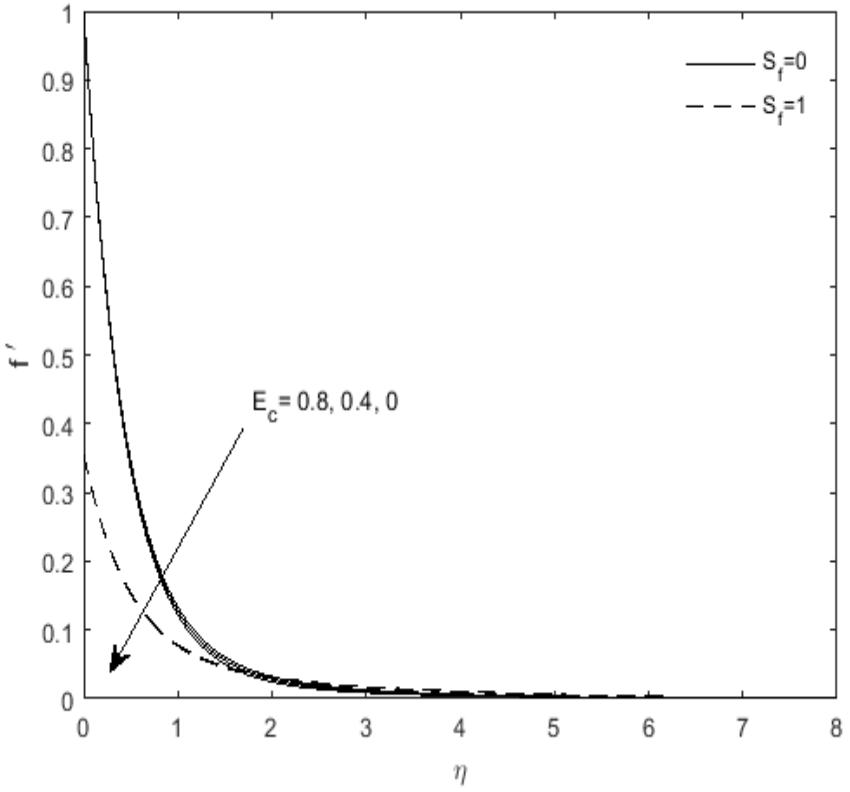

Fig.4. Velocity profile for E_c

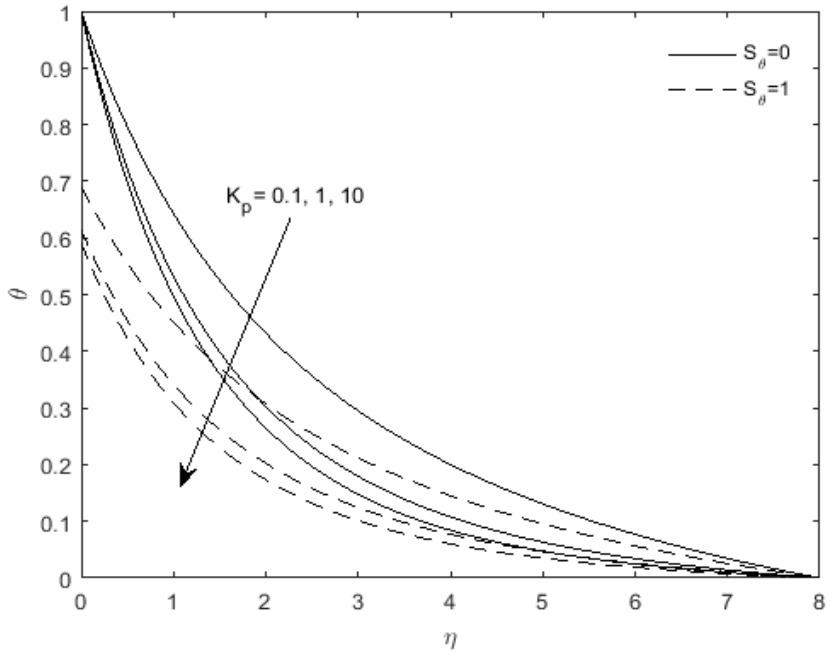

Fig.5. Temperature profile for K_p

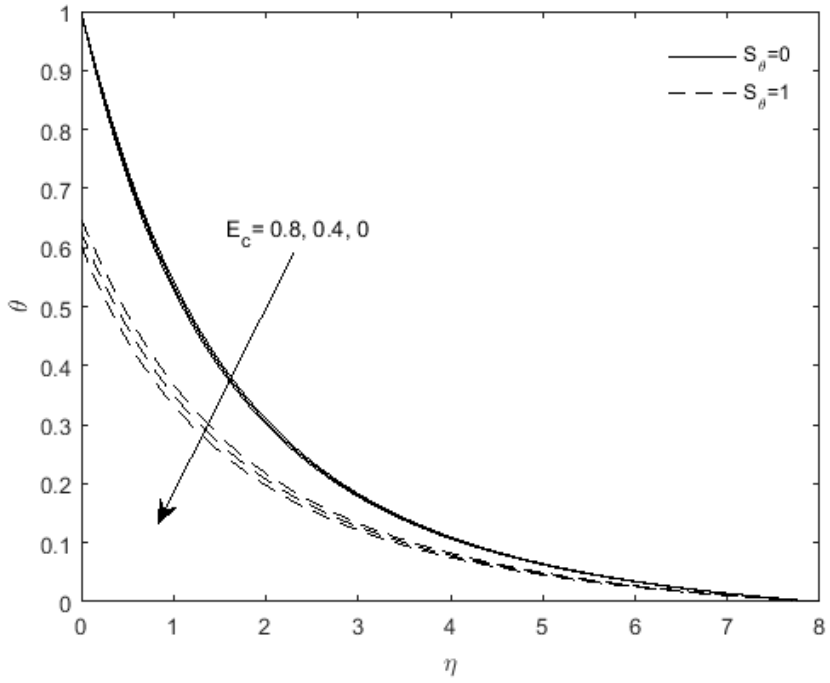

Fig.6. Temperature profile for E_c

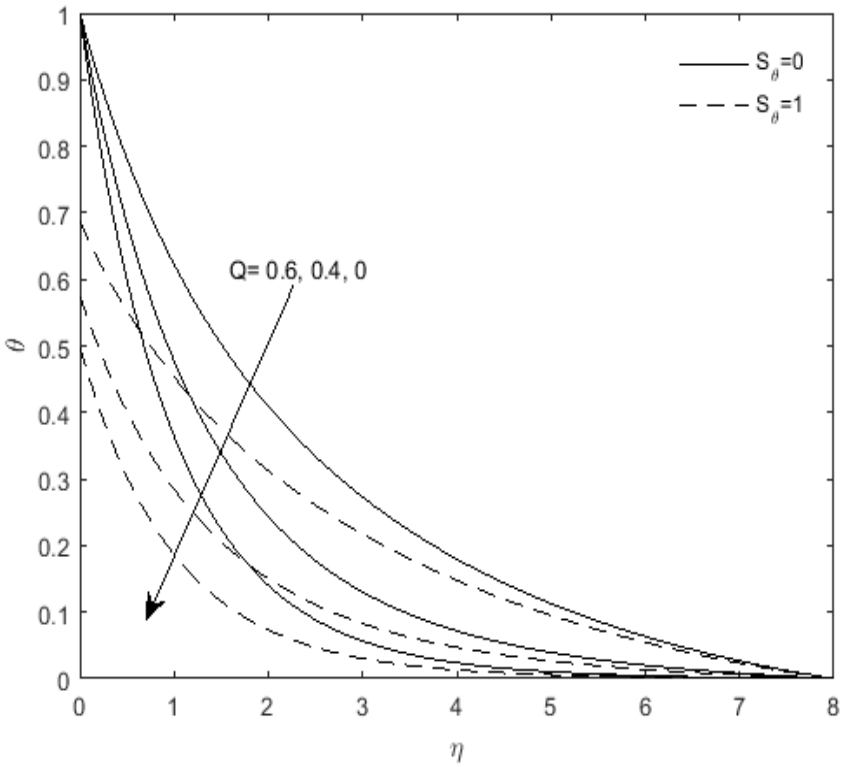

Fig.7. Temperature profile for Q

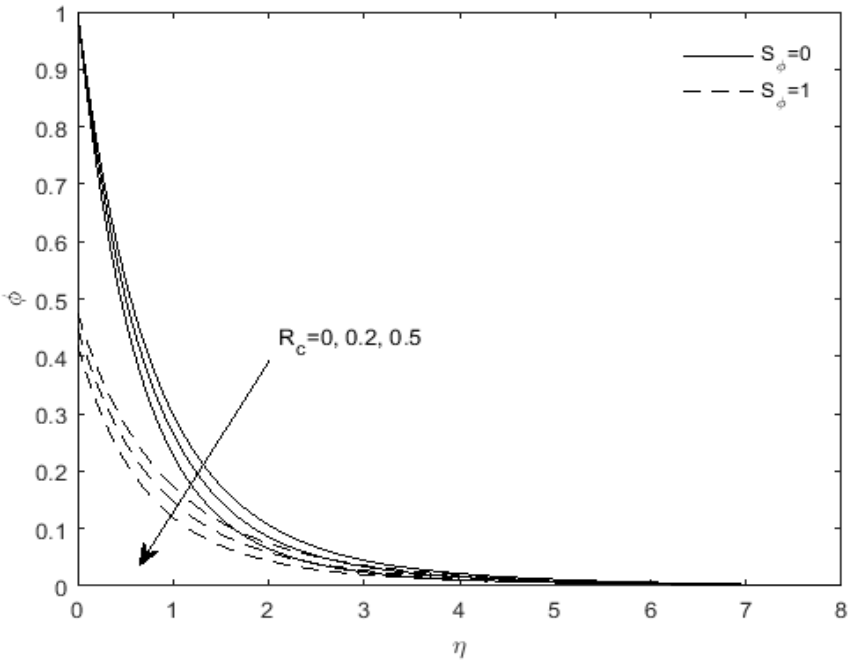

Fig.8. Concentration profile for R_c

Table

Table 1: $-f''(0)$ for different values of δ when $M = f_w = S_f = \lambda_1 = \lambda_2 = 0, K_p \to \infty$

	$-f''(0)$		
δ	Chamkha, Aly & Mansour (2010)	Mabood and Shateyi (2019)	Present result
0.8	1.261512	1.261042	1.2610428
1.2	1.378052	1.377724	1.3777241

Table 2: $-f''(0)$ for various values of M when $\delta = f_w = S_f = \lambda_1 = \lambda_2 = 0, K_p \to \infty$

	$-f''(0)$		
M	Mabood and Das (2016)	Mabood and Shateyi (2019)	Present result
0	−1.000008	−1.0000084	1.0000624
1	1.4142135	1.41421356	1.414213606
5	2.4494897	2.44948974	2.449489744
10	3.3166247	3.31662479	3.316624790
50	7.1414284	7.14142843	7.141428429

Table 3: Values of $-\theta'(0)$ when $M = f_w = S_f = S_\theta = \delta = \lambda_1 = \lambda_2 = R = 0$

	$-\theta'(0)$		
Pr	Ali (1994)	Mabood and Shateyi (2019)	Present result
0.72	0.8058	0.8088	0.809463
1	0.9691	1.0000	1.000062
3	1.9144	1.9237	1.923652
10	3.7006	3.7207	3.720631

Table-4

λ_1	λ_2	K_p	E_c	Q	R_c	S_c	$f''(0)$	$-\theta'(0)$	$-\phi'(0)$
0	0.4	1	0.2	0.5	0.5	1	-1.21798	0.54844	0.81276
0.4	0.4	1	0.2	0.5	0.5	1	-1.12895	0.56331	0.81691
0.8	0.4	1	0.2	0.5	0.5	1	-1.04472	0.57564	0.82079
0.4	1	1	0.2	0.5	0.5	1	-1.04357	0.57352	0.82050
0.4	1.5	1	0.2	0.5	0.5	1	-0.97404	0.58120	0.82341
0.4	0.4	5	0.2	0.5	0.5	1	-0.96427	0.60003	0.81996
0.4	0.4	10	0.2	0.5	0.5	1	-0.94059	0.60559	0.82040
0.4	0.4	1	0.3	0.5	0.5	1	-1.12704	0.54000	0.82336
0.4	0.4	1	0.4	0.5	0.5	1	-1.12514	0.51675	0.82978

0.4	0.4	1	0.2	1	0.5	1	-1.09941	0.36564	0.84726
0.4	0.4	1	0.2	1.5	0.5	1	-0.94533	-0.53122	0.93526
0.4	0.4	1	0.2	0.5	1	1	-1.13499	0.56215	0.87529
0.4	0.4	1	0.2	0.5	2	1	-1.14328	0.56068	0.96254
0.4	0.4	1	0.2	0.5	0.5	2	-1.14444	0.56076	0.99120
0.4	0.4	1	0.2	0.5	0.5	10	-1.16627	0.55831	1.36828